

Influence of mechanical properties of tungsten carbide–cobalt thermal spray coatings on their solid particle erosion behaviour

Y. Y. Santana*¹, J. G. La Barbera-Sosa¹, A. Bencomo¹, J. Lesage², D. Chicot², E. Bemporad³, E. S. Puchi-Cabrera^{1,4} and M. H. Staia¹

The present investigation has been carried out in order to study the erosion wear behaviour of WC–Co base thermal spray coatings. WC–12Co and WC–10Co–4Cr coatings were deposited by means of high velocity oxygen fuel (HVOF) thermal spraying. The erosion tests were conducted at impact angles of 30 and 90° using SiC particles of ~50 µm in diameter as erodent, at a velocity of 83.4 m s⁻¹. It has been found that the erosion rate for both coated systems was higher when the test was carried out at an angle of 90°. The through-thickness residual stresses of the coatings, as well as the microstructural characterisation, allowed an explanation of the results and the erosion mechanisms in each case. It has been found that, under the experimental conditions carried out in the present study, the WC–10Co–4Cr coating exhibited a higher erosive wear resistance as compared to the WC–12Co coating.

Keywords: HVOF, Thermal spray, WC–12Co and WC–10Co–4Cr coatings, Erosion, Residual stresses, Toughness

Introduction

In the past few years, due to new legislation regarding the production of electrolytic hard chromium (EHC) plating, extensive research programmes have been carried out aimed at finding appropriate alternative processes, more friendly from the environmental point of view, able to substitute such coatings in components exposed to severe wear and corrosion operating conditions.¹ Among the results of such research activities, it has been shown that WC–Co base coatings deposited by high velocity oxygen fuel (HVOF) are good candidates for such a purpose, particularly for the successful replacement of EHC in aeronautical and aerospace applications.^{2–8} HVOF WC–Co base cermets can withstand high contact pressures without spallation and are often used in applications where abrasive wear and erosion resistance are of a primary concern, whereas WC–Co–Cr base coatings are preferred when a higher corrosion resistance is required.

Mann *et al.*⁹ have shown that HVOF WC–Co base coatings can increase the slurry erosion resistance of some critical components employed in the oil industry,

such as gate valves and seat rings, which results in a significant cost reduction. However, it has also been reported that Cr addition to WC–Co based coatings improves the binding of carbides to the matrix, thereby improving the erosion resistance as compared to WC–Co base coatings.¹⁰ In this sense, Wheeler and Wood¹¹ have assessed the performance of different coatings including EHC, an electroless nickel composite and two HVOF WC coatings, as feasible candidates for use in offshore gate valves, and have concluded that deposition gun WC–10Co–4Cr thermal spray coatings could increase considerably the slurry erosion wear resistance in comparison to the other coatings.

As indicated by Bingley and O'Flynn,¹² erosive wear is a difficult process to examine and it is not surprising that no universally accepted predictive models are available. These authors have analysed the mechanical properties of a wide range of steels along with their erosion wear rates, which have been compared with the predictions of the models proposed by Hutchings^{13,14} and Sundararajan,¹⁵ applied initially for ductile materials. Bingley and O'Flynn¹² concluded that none of the models were completely satisfactory in this respect, because the choice of the experimental materials was not the best for the validation of the predictive models due to their complex microstructures and possible presence of residual stresses.

Some of the models involve in their equations two material constants: fracture toughness and hardness.^{14,16–18} For example, Wayne and Sampath¹⁸ suggested that the erosion rate of WC–Co base thermal sprayed coatings, E , was proportional to a parameter β that combines the fracture toughness K_{IC} , Vickers hardness, H_V , and Co

¹School of Metallurgical Engineering and Materials Science, Faculty of Engineering, Universidad Central de Venezuela, Apartado 49141, Caracas 1042-A, Venezuela

²Université Lille Nord de France, F-59000 Lille; USTL, LML, CNRS, UMR 8107, F-59650 Villeneuve d'Ascq, France

³University of Rome 'ROMA TRE', Mechanical and Industrial Engineering Department, Via Vasca Navale 79, 00146 Rome, Italy

⁴Venezuelan National Academy for Engineering and Habitat, Palacio de las Academias, Postal Address 1723, Caracas 1010, Venezuela

*Corresponding author, email yucelys.santana@ucv.ve

volume fraction V_f^{Co} of the material by means of a simple relationship. Accordingly

$$E = \alpha\beta \quad (1)$$

where α represents a proportionality constant and

$$\beta = K_c^{3/8} H_V^{1/2} \frac{V_f^{\text{Co}}}{1 - V_f^{\text{Co}}} \quad (2)$$

The fracture toughness considered in the above model is that measured normal to the coating/substrate interface, since in this direction it is greater than that determined along the interface, due to the low strength between the splats.

The erosion process involves stress states of a complex nature, large plastic deformations and high strain rates, which coupled with the highly heterogeneous microstructural and mechanical characteristics of thermal sprayed coatings, makes its investigation very difficult. Particularly, in the case of HVOF WC–Co base coatings, due to their brittle–ductile composite nature characterised by the presence of brittle hard carbides embedded in a soft ductile matrix, the prediction of the effects of erodent particle size and impact angle on erosion rate and mechanisms is much more difficult.¹⁹ However, due to their relevance in a number of key industrial sectors, the study of the erosion mechanisms and response of these materials to erosion wear is of utmost importance.

Therefore, the present investigation has been conducted in order to study the erosion wear behaviour of two different thermal sprayed WC base cermets with Co and Co–Cr as binders, as a function of their morphology, roughness, hardness and residual stresses, contributing in this way to the understanding of the complex phenomena just described.

Experimental techniques

WC–12Co and WC–10Co–4Cr coatings were deposited by HVOF in an industrial facility on samples of SAE 1045 steel as substrate, employing a JP-5000 deposition gun. Table 1 summarises the deposition conditions, which correspond to those typically applied at industrial level. In the as deposited condition, the coatings had a mean roughness of R_a about 6–7 μm . Subsequently, both coatings were polished in order to achieve a roughness of less than $\sim 0.2 \mu\text{m}$, as well as uniform thicknesses of ~ 350 and $500 \mu\text{m}$, for the WC–12Co and WC–10Co–4Cr coatings, respectively.

The coatings were examined by scanning electron microscopy (SEM) techniques. The observations were performed both on the cross-section and top surface (parallel to the deposition plane) of the coatings. Additionally, the average coating porosity was determined by optical microscopy and image analysis conducted on both

observation planes after careful preparation by means of standard metallographic procedures by Struers Company. The apparent porosity value reported was the average of 20 separate fields taken at a magnification of $\times 200$, as indicated in the ASTM E2109-01 standard.²⁰ The different phases present in the coatings were analysed by XRD techniques, employing a diffractometer and Cu K_α radiation. Both hardness (corresponding to 10 N normal load) and the elastic modulus of these coatings were determined by means of conventional and instrumented indentation techniques. Such results have been reported elsewhere.²¹

The through-thickness residual stress field was determined by means of the incremental hole drilling method.²² Tests were carried out using a high velocity drilling machine (Restan 44; Sint Technology, Calenzano, Italy) coupled with a coaxially assembled optical microscope for the direct measurement of the hole diameter and eccentricity, by means of a centesimal dial gauge. The mill is powered by a compressed air turbine ($P=5$ bar, $\omega=3 \times 10^5 \text{ rev min}^{-1}$), and a stepping motor electronically controlled for a single feed motion step of $1 \mu\text{m}$ generates the vertical displacement. The tests were conducted by carrying out successive drilling steps of $20 \mu\text{m}$ in depth until the substrate was reached.

After drilling, the specimens were sectioned in order to determine the coating thickness and hole depth by means of SEM observations. The first output of the hole drilling test are the relaxation strain/depth curves, from which it is possible to compute the through-thickness residual stress variation, provided that correct values for the calibration coefficients are employed. Such coefficients were determined by means of the Integral Method,²² which has been explained in detail elsewhere.²³

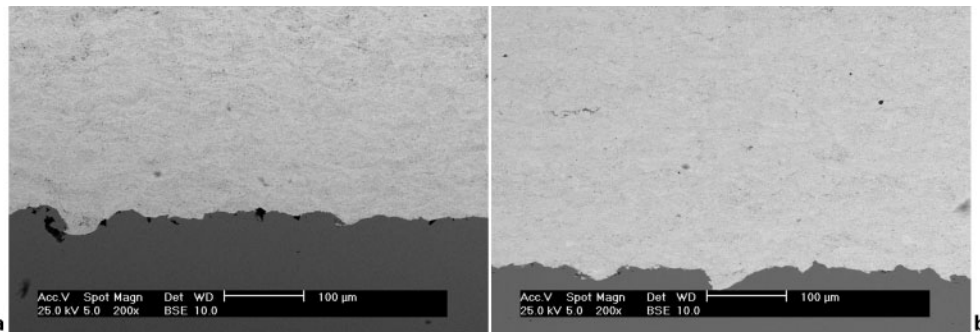
The determination of the fracture toughness of the WC base coatings was carried out by indentation tests conducted on the cross-section of the deposits. For this purpose, a CSM Revetest, under constant load conditions, was employed. A load of 100 N was applied to the material and the indentations were carried out along the centreline of the coatings, ensuring that one of the diagonals was parallel to such a direction. For this load applied, both diagonals were less than 50% of the coating thickness. For the determination of the fracture toughness, only those cracks parallel to the coating/substrate interface were taken into account. The length of such cracks was measured on optical photomicrographs. For cracks of a median radial type, the crack length c is given by¹⁶

$$c = \frac{a_{//} + a_{\perp}}{4} + \frac{l_1 + l_2}{2} \quad (3)$$

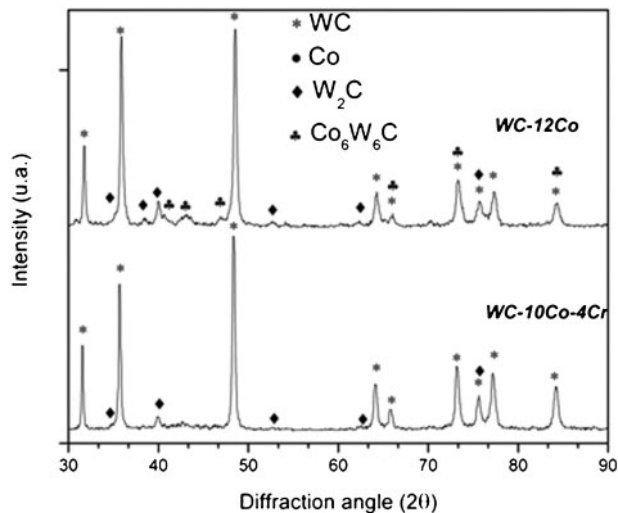
In this equation, the parameters $a_{//}$ and a_{\perp} represent the indent diagonals parallel and normal to the interface respectively, whereas l_1 and l_2 represent the length of the

Table 1 Deposition parameters of HVOF process

	WC–10Co–4Cr	WC–12Co
Thermal spray gun	TAFA HVOF JP-5000	TAFA HVOF JP-5000
Spraying distance/mm	300	380
Spraying angle/ $^\circ$	90	90
Powder feeding rate/g min^{-1}	40	83
Particle size/ μm	45–55	22–66
Kerosene flux/L min^{-1}	10	23
Oxygen flux/L min^{-1}	35	78



1 SEM images of cross-section of coatings: a WC-12Co; b WC-10Co-4Cr



2 XRD spectra of WC-12Co and WC-10Co-4Cr coatings

cracks formed at the corners of the diagonal parallel to the interface, which also are parallel to it. If a Palmqvist type cracking condition occurs, the crack length is simply given by the mean values of l_1 and l_2 .

The well known equation proposed by Ponton and Rawlings²⁴ for WC-Co materials was used to calculate the fracture toughness, which was determined under the assumption that crack morphology was of a median radial type, since the ratio of the crack length to the mean of the indent diagonals $cla=2.06$.²⁴ Therefore, the model advanced by Evans and Davis²⁴ was applied for the computation of such a property. On the other hand, the determination of the fracture toughness of the WC-12Co coating was carried out by means of the model advanced by Niihara *et al.*,²⁴ since the cracks generated from the indentation were found to present a Palmqvist geometry type, with a ratio $lla=0.88$.²⁴

The erosion tests were carried out in dry environment at room temperature, according to the ASTM G76-05 standard.²⁵ For this purpose, sharp SiC particles of $\sim 50 \mu\text{m}$ in diameter, fed at a rate of 2 g min^{-1} with filtered compressed air at a pressure of 140 kPa, were

employed. The particles impacted the coatings at angles of 30 and 90°. The steady state erosion rate was monitored as a function of time. The mean erosion rate ($\text{mm}^3 \text{ g}^{-1}$) was computed as the steady state erosion rate (mg min^{-1}) per unit of abrasive particles mass (g min^{-1}), divided by the density of the sample (g cm^{-3}). The density value employed for the WC-Co base coatings was of $\sim 14.7 \text{ g cm}^{-3}$.²⁶ The particles impact velocity has a value of 83.4 m s^{-1} and was determined by employing the model advanced by Ninham and Hutchings.²⁷

Experimental results

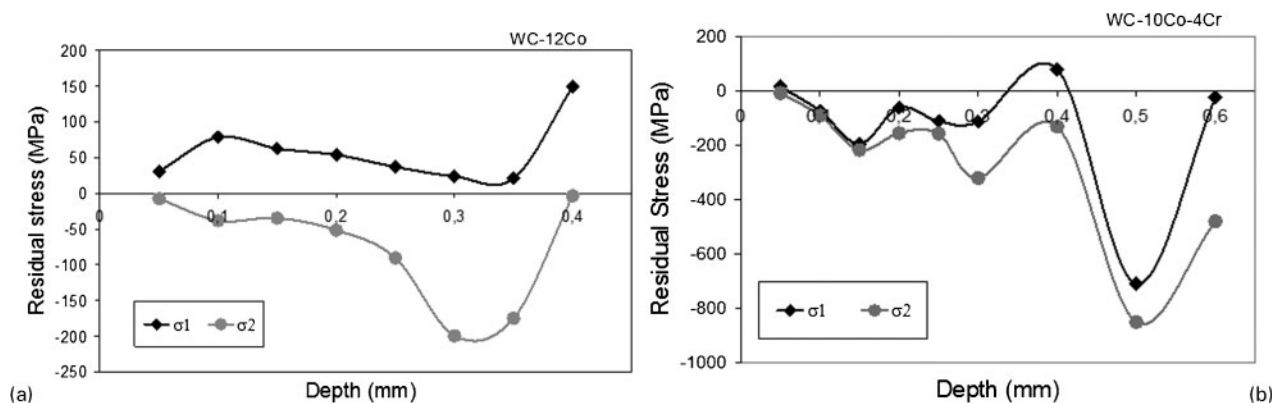
The microstructural study of the WC-10Co-4Cr and WC-12Co coatings indicated that these present a uniform and dense morphology. Therefore, as shown in Fig. 1, the typical microstructure composed of superposed and oriented lamellas parallel to the coating/substrate interface is not at all evident. The dense microstructure of the coatings was also corroborated by measuring the apparent porosity, which was found to be less than 1%, both on the cross-section and surface of both deposits.

Figure 2 on the other hand, shows the results of the XRD analysis of both thermal sprayed coatings. The results indicate that decarburisation of the WC phase has taken place, due to the formation of the deleterious brittle W_2C phase. This analysis also allowed the evaluation of the decarburisation degree, an important parameter that should be taken into account in the interpretation of the wear behaviour of the coatings. According to Savarimuthu *et al.*,⁸ the best results regarding the wear behaviour of these coatings is attained if minimum decarburisation takes place. The ratio of the peak heights $\text{W}_2\text{C}/\text{WC}$ for the WC-10Co-4Cr and WC-12Co coatings were found to be of approximately 5.5 and 11.4% respectively, indicating that the WC-12Co coating undergoes more decarburisation.

Table 2 presents the Vickers hardness values H_V obtained on the cross-section of the coatings, by applying a load of 9.8 N, as well as the values of elastic modulus E determined from Berkovich instrumented

Table 2 Mechanical properties of investigated coatings

Coating	H_{IT}/E	H_V/GPa	H_{IT}/GPa	E/GPa	$K_C/\text{MPa m}^{1/2}$
WC-10Co-4Cr	0.043	11.3 ± 0.8	12.1 ± 2.1	261 ± 10	1.42 ± 0.80
WC-12Co	0.032	7.3 ± 0.9	8.1 ± 1.1	254 ± 12	4.56 ± 0.90



3 Through-thickness residual stress profiles of coatings: a WC-12Co; b WC-10Co-4Cr

indentations, ratio of instrumented hardness to elastic modulus H_{IT}/E and fracture toughness. Here, it is observed that the fracture toughness value of the WC-12Co coating is greater than that of the WC-10Co-4Cr deposit, in agreement with the results earlier reported by López-Cantera and Mellor,¹⁶ as well as by Lima *et al.*²⁸

Figure 3 shows the residual stress profiles that were determined for the WC-12Co and WC-10Co-4Cr coatings, which are described in terms of the change of the maximum (σ_1) and minimum (σ_2) values of the stress components with depth. For the WC-12Co coating, it can be observed that σ_1 is of a tensile nature, from the surface of the deposit up to the coating/substrate interface. On the contrary, σ_2 is of a compressive nature, whose largest magnitude is achieved near the interface. Through the thickness of the coating, the magnitude of σ_1 is always greater than that of σ_2 , except near the interface. For the WC-10Co-4Cr coating, as shown in Fig. 3b, both components of the residual stress state are mainly of a compressive nature, with the exception of the change observed in σ_1 at a depth of 400 μm , which achieved a tensile value of 78 MPa. At the interface, σ_1 and σ_2 achieved their highest compressive magnitudes of 709 and 850 MPa respectively.

Table 3 presents the results of the evaluation of the parameters that quantify the erosive wear behaviour of both coatings, including the mean erosive wear rate and erosion wear resistance. In both cases, wear achieved a steady state, with larger values of the erosion rate for the WC-12Co coating than for the WC-10Co-4Cr deposit, in the range of 33 and 15%, for impact angles of 90 and 30° respectively. Figures 4 and 5 illustrate the SEM observations of the wear scars of both coatings, for both impact angles. Here, it can be clearly seen that for the tests carried out at an impact angle of 30° (Fig. 4), the morphology of the wear scars of both coatings can be described as consisting of grooves and cracks, whereas for the angle of 90° (Fig. 5), both coatings exhibit carbide fracture and particle removal with formation of deeper craters. The

EDS analysis conducted at the centre of the scars (Fig. 5) did not show the presence of Fe, which corroborates that the wear process occurs only on the coating.

Discussion

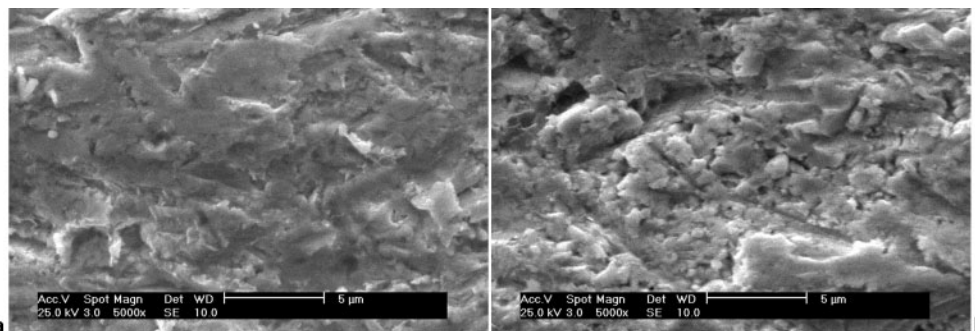
Regarding the erosive wear mechanisms, it is well known that ductile and brittle materials exhibit significantly different behaviours when the erosion rate is determined as a function of the impact angle. The results obtained in the present investigation show that the mean erosion rates of the WC-10Co-4Cr and WC-12Co coatings impacted at an angle of 90° are 32 and 46% greater respectively than those determined at an impact angle of 30°. Such a trend tends to indicate that the WC base coatings exhibit a brittle erosive wear mechanism, as suggested by Hussainova.²⁹

Ball and Patetson³⁰ have reported that the Co content at which the transition from brittle wear to ductile wear takes place is in the range of 10%, whereas according to Wright *et al.*,³¹ such a transition occurs at approximately 7%. Taking into consideration these previous findings, the coatings under investigation, which have a Co content of 10 and 12 wt-%, should exhibit a ductile wear mechanism. However, the deposits showed an increased worn volume at an impact angle of 90° than at 30°, which would indicate that the wear mechanism is partially brittle.

In this sense, other authors³²⁻³⁵ have reported that WC base compounds exhibit a combined or mixed ductile-brittle erosive wear mechanism, in agreement with the SEM observations presented in Figs. 4 and 5. This experimental evidence shows that, once the steady state is achieved, the mixed wear mechanism exhibited by both coatings involves the plastic deformation of the binding phase, characterised by the presence of grooves, and the fracture and subsequent removal of the WC particles. At relatively low impact angles (30°), the ductile wear mechanism of the coatings is more noticeable and characterised by the extrusion or plastic deformation of

Table 3 Mean erosive wear rate and erosion resistance for WC-10Co-4Cr and WC-12Co coatings

Coating	V_f^{Co}	β	Mean erosive wear rate/ $\text{mm}^3 \text{g}^{-1}$			
			Impact angle	30°	90°	Wear resistance/ g mm^{-3}
WC-12Co	0.33±0.01	2.68	0.156±0.006	0.289±0.021	6.40±0.23	3.45±0.25
WC-10Co-4Cr	0.36±0.01	1.88	0.133±0.008	0.195±0.018	7.52±0.45	5.12±0.47



4 SEM images of erosion wear scars on surface of coatings impacted by small SiC particles at an angle of 30°: a WC-10Co-4Cr; b WC-12Co

the Co matrix, whereas just a small difference in the mean erosion rate of both deposits can be observed.

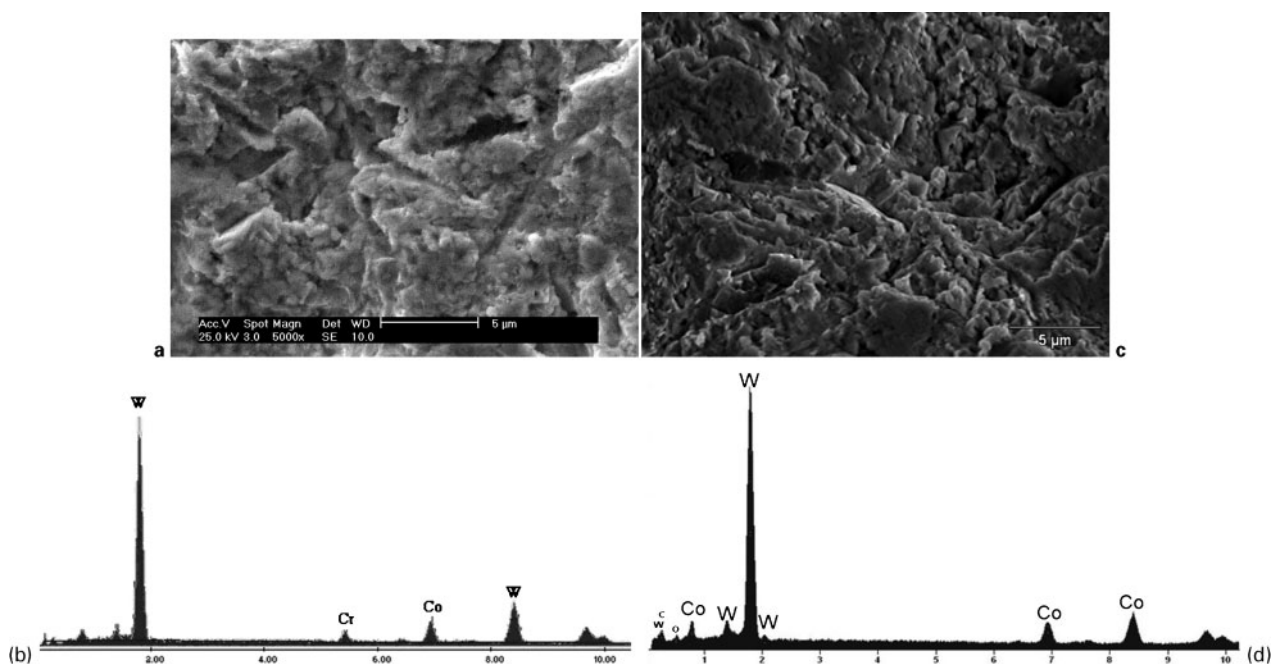
On the other hand, for the tests carried out at an impact angle of 90°, the results indicate that the WC-10Co-4Cr coating exhibits a good behaviour against erosive wear induced by small particles, in comparison with the behaviour showed by the WC-12Co coating. In this sense, some authors^{10,36} have proposed that the good tribological behaviour of the WC-Co-Cr base coatings is due to the presence of Cr in the binding phase, which provides a higher mechanical strength and hardness. Thus, the wear mechanism could be governed by the binder strength, since the erosive particles could impact in isolated regions of the binder phase, enhancing the removal of the materials. A similar analysis has been reported by Dent *et al.*³⁷ regarding the evaluation of the erosive wear resistance that WC-12Co coatings oppose to small alumina particles.

As suggested by Wada and Ritter,³⁸ the erosion mechanism of the WC-Co base coatings under investigation could also be related to the characteristics (size and type) of the impacting particles. As indicated previously, in the present investigation, the erosive wear behaviour was analysed employing SiC particles with hardness greater than that of the worn material (WC-Co). In this

case, it would be expected that the erosion mechanism would be controlled by the formation and propagation of microcracks within the WC grains, particularly in the tests conducted at an impact angle of 90°. Thus, in agreement with the observations of previous authors,³⁸⁻⁴¹ the fracture toughness would have an important effect on the erosion rate. From the data presented in Table 2, it can be observed that there is not any correlation between the erosive wear rate and fracture toughness of the coatings, also in agreement with the results reported by other researchers,^{29,35} who have determined that the erosive wear rate is more dependent on the hardness of both impacting particles and impacted target.

Thus, in an attempt to analyse the present erosion wear results on the basis of the model advanced by Wayne and Sampath,¹⁸ Table 3 includes the values of the parameter β (equation (2)) obtained for both coatings. Here, it can be observed that for the WC-12Co and WC-10Co-4Cr thermal sprayed coatings, the model provides a good trend for both impact angles, in the sense that, as β increases the erosion rate also increases.

The behaviour of the coatings against erosive wear could also be analyzed on the basis of the ratio H_{IT}/E , presented in Table 2. As indicated by some authors,^{16,41}



5 SEM images and EDS analysis of erosion wear scars on surface of coatings impacted by small SiC particles at angle of 90°: a, b WC-10Co-4Cr; c, d WC-12Co

as such a ratio increases, the resistance to erosive wear is also expected to increase. In the present investigation, it has been found that the WC–10Co–4Cr coating presents a higher resistance to erosive wear than the WC–12Co deposit (Table 3), which correlates with its higher H_{IT}/E ratio.

Also, it could be suggested that a larger amount of the brittle W_2C phase found in the WC–12Co coating, in comparison with that found in the WC–10Co–4Cr deposit, would impair the resistance to erosive wear, since the presence of such a phase decreases the strength of the coating, leading to an increase in the brittle erosive wear mechanism.²⁶ The present results can also be interpreted in terms of the residual stress profiles of the coatings. As shown in Fig. 3b, the WC–10Co–4Cr coating is under a compressive residual stress state, with a mean value in the range of -200 MPa, from the surface up to a depth of approximately $300\ \mu\text{m}$. Such stress state would allow an explanation of the decrease in the contribution of the brittle erosive wear mechanism that has been observed for this material at an impact angle of 90° .

Conclusion

The erosion rate of the thermal sprayed WC–Co base coatings that have been studied is more severe when the material is impacted by solid particles at an angle of 90° , in comparison with an angle of 30° . The erosive wear mechanism is a combination of ductile and brittle mechanisms. The WC–10Co–4Cr coating exhibited a higher resistance to erosive wear, in the range of approximately 15 and 31%, in comparison with the WC–12Co deposit, when both materials are impacted by small solid particles at angles of 30 and 90° respectively. This result has been attributed to smaller content of the decarburised brittle W_2C phase, as well as the presence of compressive residual stresses through the coating thickness. The ratio of hardness to elastic modulus is an appropriate parameter as far as the correlation with the erosive wear rate of the coating is concerned. As such a ratio increases, the erosive wear rate of the coating due to the impact of small SiC particles decreases. Thus, the WC–10Co–4Cr coating, with a higher hardness to elastic modulus ratio, exhibits a smaller erosive wear rate than the WC–12Co coating.

Acknowledgements

The authors gratefully acknowledge the financial support provided by the Postgraduate Cooperative Programme (PCP) between the France and Venezuela (FONACIT). Also, Y. Y. Santana acknowledges the financial support of CDCH-UCV through the project no. PI 08-00-5792-2005. M. H. Staia acknowledges the financial support of FONACIT through the project no. UCV F-2001000600. The Department of Chemical and Materials Engineering, University of Rome 'La Sapienza', and especially Professor T. Valente, are also deeply acknowledged.

References

- Official Journal of the European Union: 'Directive 2000/53/EC of the European Parliament and of the Council of 18 September 2000 on end-of life vehicles', L 269/34, Official Journal of the European Communities, Brussels, Belgium, 2000.
- E. W. Brooman: 'Wear behavior of environmentally acceptable alternatives to chromium coatings: nickel-based candidates', *Met. Finish.*, 2004, **102**, (9), 75–82.
- B. D. Sartwell, K. O. Legg, J. Zimmerman, M. Reynolds, A. Drennan, J. Gribble, J. Magno, R. Mason and A. Kaltenhauser: 'Validation of HVOF thermal spray coatings as replacements for hard chrome plating on hydraulic/pneumatic actuators', Final report, NRL, Washington, DC, USA, 2006.
- B. D. Sartwell, D. Dull, J. Falkowski, K. O. Legg, P. Bretz, J. Schell, J. Devereaux, J. Sauer, C. Edwards, P. Natishan and D. Parker: 'Validation of WC/Co and WC/CoCr HVOF thermal spray coatings as a replacement for hard chrome plating on aircraft landing gear', NRL report no. XYZ, NRL, Washington, DC, USA, 2002.
- M. Dorfman, J. DeFalco and J. Karthikeyan: Proc. 1st Int. Thermal Spray Conf., Montreal, Que., Canada, May 2000, ASM International, 471–478.
- R. T. R. McGrann, D. J. Greving, J. R. Shadley, E. F. Rybicki, T. L. Kruecke and B. E. Bodger: *Surf. Coat. Technol.*, 1998, **108–109**, 59–64.
- L.-M. Berger, W. Hermel, P. Vuoristo, T. Mantyla, W. Lengauer and P. Eitmayer: 'Structure, properties and potentials of WC–Co, Cr_3C_2 –NiCr and TiC–Ni-based hard metal-like coatings', Proc. 9th Natl Thermal Spray Conf.: 'Thermal spray: practical solutions for engineering problems', Cincinnati, OH, USA October 1996, ASM International, 89–96.
- A. C. Savarimuthu, I. Megat, H. F. Taber, J. R. Shadley, E. F. Rybicki, W. A. Emery, J. D. Nuse and D. A. Somerville: 'Sliding wear behavior as a criterion for replacement of chromium electroplate by tungsten carbide (WC) thermal spray coatings', Proc. 20th Oklahoma AIAA/ASME Symposium: 'Aircraft applications', Stillwater, OK, USA, February 2000, AIAA/ASEM, 1095–1104.
- B. S. Mann, V. Arya, A. K. Maiti, M. U. B. Rao and P. Joshi: *Wear*, 2006, **260**, 75–82.
- J. K. N. Murthy, D. S. Rao and B. Venkataraman, *Wear*, 2001, **249**, (7), 592–600.
- D. W. Wheeler and R. J. K. Wood: *Wear*, 2005, **258**, 526–536.
- M. S. Bingley and D. J. O'Flynn: *Wear*, 2005, **258**, 511–525.
- I. M. Hutchings: *Wear*, 1981, **70**, 269–281.
- I. M. Hutchings: 'Tribology: friction and wear of engineering materials', 1992, London, Edward Arnold.
- G. Sundararajan: *Wear*, 1991, **149**, 129–153.
- E. López-Cantera and B. G. Mellor: *Mater. Lett.*, 1998, **37**, 201–210.
- H. C. Meng and K. C. Ludema: *Wear*, 1995, **181–183**, 443–457.
- S. F. Wayne and S. Sampath: *J. Therm. Spray Technol.*, 1992, **1**, (4), 307–315.
- R. G. Rateick, Jr, K. R. Karasek, A. J. Cunningham, K. C. Goretta and J. L. Routbort: *Wear*, 2006, **261**, 773–778.
- 'Test methods for determining area percentage porosity in thermal sprayed coatings', E2109-01, ASTM, West Conshohocken, PA, USA, 2001.
- Y. Y. Santana, J. G. La Barbera-Sosa, J. Caro, E. S. Puchi-Cabrera and M. H. Staia: *Surf. Eng.*, 2008, **24**, (5), 374–382.
- T. Valente, C. Bartuli, M. Sebastiani and A. Loreto: *J. Therm. Spray Technol.*, 2005, **14**, (4), 462–470.
- Y. Y. Santana, J. G. La Barbera-Sosa, M. H. Staia, J. Lesage, E. S. Puchi-Cabrera, D. Chicot and E. Bemporad: *Surf. Coat. Technol.*, 2006, **201**, 2092–2098.
- C. B. Ponton and R. D. Rawlings: *Mater. Sci. Technol.*, 1989, **5**, 865–872.
- 'Standard test method for conducting erosion test by solid particle impingement using gas jets', G76-05, ASTM, West Conshohocken, PA, USA, 2005.
- H. M. Hawthorne, B. Arsenault, J. P. Immargeon, J. G. Legoux and V. R. Parameswaran: *Wear*, 1999, **225–229**, 825–834.
- A. J. Ninham and I. M. Hutchings: 'A computer model for particle velocity calculation in erosion testing', Proc. 6th Int. Conf. on 'Erosion by liquid and solid impact', 50-1/50-7; 1983, Cambridge, Cavendish Laboratory.
- M. M. Lima, C. Godoy, J. C. Avelar-Batista and P. J. Modenesi: *Mater. Sci. Eng. A*, 2003, **A357**, 337–345.
- I. Hussainova: *Wear*, 2005, **258**, 357–365.
- A. Ball and A. W. Patetson: 'Microstructural design of erosion resistance of hard metals', Proc. Int. Conf. on 'Recent developments in special steels and hard metals', Rhode Island, 1985, 377–391.
- I. G. Wright, D. K. Shetty and A. H. Clauer: Proc. 6th Int. Conf. on 'Erosion by liquid and solid impact', (ed. J. E. Field and N. S. Corney), 1–63; 1983, Cambridge, Cavendish Laboratory.

32. R. G. Rateick, Jr, K. R. Karasek, A. J. Cunningham, K. C. Goretta and J. L. Routbort: *Wear*, 2006, **261**, 773–778.
33. G. Östberg, K. Buss, M. Christensen, S. Norgrem, H.-O. André, D. Mari, G. Wahnström and I. Reineck: *Int. J. Refract. Met. Hard Mater.*, 2006, **24**, 145–154.
34. I. M. Hutchings: 'Solid particle erosive wear testing', in 'ASM handbook', Vol. 8, 'Mechanical testing and evaluation', 728–751; 2000, Materials Park, OH, ASM International.
35. Z. Feng and A. Ball: *Wear*, 1999, **233–235**, 674–684.
36. A. Karimi, Ch. Verdon, J. L. Martin and R. K. Schmid: *Wear*, 1995, **186–187**, 480–486.
37. A. H. Dent, S. de Palo and S. Sampath: *J. Therm. Spray Technol.*, 2002, **11**, (4), 551–558.
38. S. Wada and J. E. Ritter (eds.): 'Erosion of ceramic materials', 71; 1992, Zurich, Trans Tech Publications.
39. I. Hussainova: *Tribology Int.*, 2001, **34**, 89–93.
40. C. Dogan and J. Hawk: *Wear*, 1999, **225–229**, 1050–1058.
41. A. Leyland and A. Matthews: *Wear*, 2001, **246**, (1–2), 1–11.